A FRONT-TO-BACK-END MODELING OF *I/Q* MISMATCH EFFECTS IN A COMPLEX-IF RECEIVER FOR IMAGE-REJECTION ENHANCEMENT

Pui-In Mak [1], Seng-Pan U [2] and R.P. Martins [3]

Mixed-Signal VLSI Laboratory (MSVLSI)
Faculty of Science and Technology, University of Macau, Av. Padre Tomás Pereira S.J., Taipa, Macau SAR, China
E-mails : 1 - p.i.mak@ieee.org, 2 - benspu@umac.mo, 3 - rmartins@umac.mo
3 - On leave from Instituto Superior Técnico (IST), Lisbon, Portugal

ABSTRACT

Insufficient image-rejection due to *I/Q* mismatch limits complex-IF receivers' application in modern wireless communication systems. This paper proposes a new modeling method to effectively enhance such kind of receiver image-rejection performance, through an understanding of the correlation between the different image-reject functional blocks. The presented complex-IF receiver mainly consists of a Double Quadrature Down-Converter (DQDC) and an Analog-Double Quadrature Sampling (A-DQS) scheme for the frequency down-conversions. Systematic analysis of the *I/Q* mismatch issues will be presented first. Then, according to the analyzed results and assuming that the total required image-rejection is 70dBc, an optimum combination of allowable mismatch in the functional blocks is obtained as an example for DCS1800 application. Such combination is verified through non-ideal behavioral simulations and is further discussed in terms of its practicability in CMOS implementation.

Keywords: Double quadrature sampling/down-conversion, DCS1800, *I/Q* mismatch, image-rejection, complex-IF receiver

1. INTRODUCTION

Complex-IF wireless receiver topology [1-4] is attracting more attention recently for its high capacity of integration and low-power consumption, since the image problem is tackled by *signal cancellation*. Thus, power-hungry off-chip image-rejection filters can be eliminated. However, the successfulness of such cancellation method is highly dependent on the matching precision between the in-phase *(I)* and quadrature *(Q)* channels. To relax the channels matching precision while still achieving high image-rejection, various RF and IF on-chip image-reject functional blocks, such as passive or active polyphase filters [1] and image-rejection mixers [2-4] can be cascaded to suppress the image continually in the Analog Front-End (AFE). Regrettably, in terms of power consumption, noise figure and occupied chip-area, the order of such functional blocks must be balanced with the corresponding savings that they allow. In this paper, we developed a new modeling method based on the analysis of the correlation among different image-reject functional blocks in the receiver. The architecture of the complex-IF receiver that will be analyzed is presented in Fig. 1, mainly consisting of a Double Quadrature Down-Converter (DQDC) front-end [1] followed by Analog-Double Quadrature Sampling (A-DQS), for the RF-to-IF and IF-to-Baseband frequency down-conversions, respectively. The superiorities of such receiver are: 1) the DQDC possesses an excellent image-rejection even with moderate phase and gain matching accuracy throughout the *I* and *Q* channels. This is due to the suppression of the image interference twice, one by the quadrature generator and the other by the quadrature mixers; 2) The A-DQS scheme not only performs IF-sampling, but also can serve as an IF-to-baseband down-converter prior to the A/D conversion. Thus, when an oversampling sigma-delta ($\Sigma\Delta$) A/D converter is employed for digitization, the original required bandpass noise shaping can be replaced by its lowpass counterpart [5]. Obviously, the efficiency of noise shaping would be doubled since the
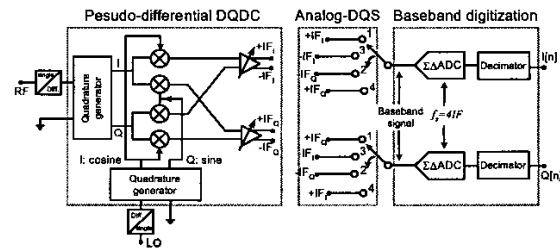

Figure 1. Modeled complex-IF receiver

efficiency of bandpass noise shaping is only half of the lowpass one. Both mentioned benefits are highly desirable in the design and implementation of a wireless receiver.

The description of this work starts by Section 2, where the mismatch issues are introduced first. Followed by the presentation of the optimum combination of mismatches and non-ideal model simulation in Section 3. Practical considerations about those results in CMOS implementation will be discussed in Section 4, and conclusions will be drawn in Section 5.

2. *I/Q* IMBALANCE MODELS OF IMAGE-REJECT FUNCTIONAL BLOCKS

2.1. Assumptions

1) The modeled receiver is basically focused on narrowband wireless communication systems, such as GSM. The circuit non-idealities such as: *KT/C* noise, DC offset, finite gain and bandwidth of amplifiers are assumed to be signal independent and will not be modeled, since they exist in both channels, resulting in no influence in the matching and, consequently, no degradation of the image-rejection performance.

2) Since the definition of image-rejection ratio (IRR) is the ratio between the signal and the image powers, which will become infinity for null *I/Q* mismatch, to ease the plotting of IRR variations, the 3-dimensional figures in the following sections will be plotted with an additional assigned mismatch (<0.001%).

2.2. Double Quadrature Down-Converter (DQDC)

2.2.1. Passive quadrature generator

To generate a high precision matched *I/Q* component in RF with reasonable power consumption, a passive quadrature generator constructed by an N-Cells cascaded *RC-CR* network, as shown Fig. 2, is usually a wise choice. Through this generator both input signal frequency bands will be filtered, therefore implying that the mandatory matching accuracy of the image-rejection mixers that will follow it can be highly relaxed. However, the penalties are: 1) Large current will be driven from the input buffer to drive the relatively low-resistive input impedance of such network; 2) Due to finite *Q*-factor of those passive *RC* elements and process fabrication variations, an over-designed cascaded *RC-CR* network is usually needed to enlarge the rejection band and reduce the sensitivity of its efficiency to the *RC* variations. Moreover, since the signal power dropped by 3dB per order, power-hungry output buffers are also required to
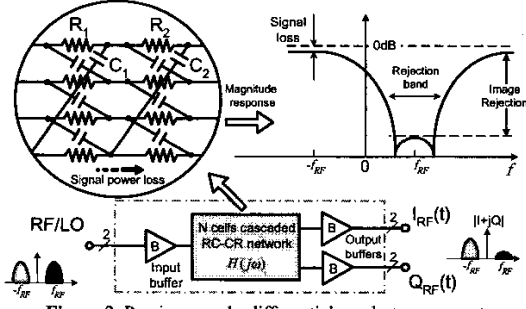
Figure 2. Passive pseudo-differential quadrature generator

compensate such losses. Obviously, the required order of the RC-CR network should be well determined to minimize the power consumption and, simultaneously, provide sufficient image-rejection. Suppose that the image-rejection of the quadrature generator is modeled as $H(j\omega)|_{\omega=2\pi f_{RF}}$, and a 2nd-order RC network is applied. Then, the IRR will be given by

$$IRR = \frac{1}{|H(j\omega)|_{\omega=2\pi f_{RF}}|^2} \qquad (1)$$

Where $H(j\omega)$ is [6]

$$H(j\omega) = \frac{(1+\omega R_1 C_1)(1+\omega R_2 C_2)}{1-\omega^2 R_1 R_2 C_1 C_2 + j\omega(R_1 C_1 + R_2 C_2 + 2R_1 C_2)} \qquad (2)$$

Note that $H(j\omega)$ is a complex frequency transfer function and in order to reject the image band accurately, f_{RF} is set in the middle between the transmission zeros, and its value is

$$f_{RF} = \frac{r_R r_C + 1}{4\pi R_1 C_1} \qquad (3)$$

Where $r_R = R_1/R_2$, $r_C = C_1/C_2$, which will lead to the following expression for $H(j\omega)|_{\omega=2\pi f_{RF}}$

$$H(j\omega)|_{\omega=2\pi f_{RF}} = \frac{(1+\frac{r_R r_C+1}{2})(1+\frac{r_R r_C+1}{2r_R r_C})}{1-\frac{(r_R r_C+1)^2}{4r_R r_C} + j\frac{r_R r_C+1}{2}(1+\frac{1}{r_R r_C}+\frac{2}{r_C})} \qquad (4)$$

Interestingly, the IRR is directly related to only the ratio of the capacitors and resistors in the two stages. Therefore, once the f_{RF}, r_R and r_C are given, the IRR at f_{RF} can be immediately obtained.
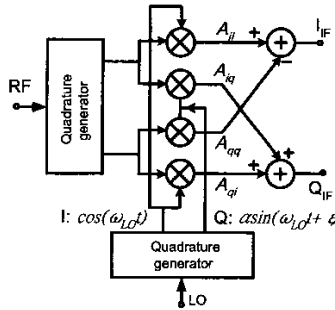

Figure 3. Non-ideal model of DQDC

2.2.2. Quadrature local oscillator

The non-ideal model of the DQDC is shown in Fig. 3, where the I and Q LO signals are generated by the other passive quadrature generator constructed by the RC-CR network. The imbalances of such LO signals' gain and phase are modeled as: I: $cos(\omega_{LO}t)$ and Q: $a\ sin(\omega_{LO}t+\varepsilon)$, where a and ε are the relative mismatches between the amplitude and phase of the quadrature local oscillator, respectively. Again, its performance depends on the order of the RC-CR network $H(j\omega)$ as

$$\alpha = |H(j\omega)|_{\omega=2\pi f_{LO}}|, \qquad \varepsilon = \angle H(j\omega)|_{\omega=2\pi f_{LO}} \qquad (5a\text{-}b)$$

2.2.3. Double quadrature mixer

For complex-to-complex frequency down-conversion, a double quadrature structure constructed by four mixers driven by the quadrature local oscillator is mandated, as shown in Fig. 3 also. Comparing with nominal real-to-complex frequency down-conversion, the variance of the mismatch is greater since it employs two more mixers. Therefore, in this paper, the amplitude mismatches (denoted as A_{ii} A_{iq} A_{qi} and A_{qq}) of the four mixers are modeled and their contribution to IRR is given by [6]

$$IRR = \left(\frac{A_{ii}+A_{qi}+A_{iq}+A_{qq}}{A_{ii}-A_{qi}-A_{iq}+A_{qq}}\right)^2 \qquad (6)$$

For the phase mismatch, the crosstalk is approximately [3]

$$IRR = \tan(\Delta\Phi) \approx \frac{\omega_{LO}}{\omega_{BW}} \cdot \frac{\Delta\omega_{BW}}{\omega_{BW}} \qquad (7)$$

where $\Delta\Phi$ is the phase mismatch, ω_{BW} is the input bandwidth of the mixers, ω_{LO} is the frequency of the local oscillator. Obviously, the phase mismatch can be highly reduced as long as the mixers are designed to have a large input bandwidth. Therefore, this mismatch effect is not as critical as the gain mismatch and it is not modeled in this paper to simplify the description of this analysis. The mismatches of the summation, subtraction and amplification functions of the DQDC are also ignored, since they are relatively uncritical for two reasons: 1) the image is already suppressed twice in the RF, first by the quadrature generator and second by the double quadrature mixers; 2) Those functions are operating at the IF, a relatively low frequency, then, high precision matching is simpler to achieve by enlarging the size of the components and symmetric layout during the implementation.

2.2.4. Overall DQDC

Summarizing the previous analysis, after simplification and under the assumption that the high-side injection frequency components generated by the mixers are totally filtered, will allow the determination of a simplified close-form expression of the image-rejection ratio (IRR) of the entire DQDC, which is given by (8). Here, for simplification, the magnitudes of signals A and B are normalized to unity and some assigned extra symbols were used, such as: $\beta=(1+A)^2$, $\lambda=(1-A)^2$, $\eta=(1+\alpha)$ and $\mu=(1-A^2)$. From equation (8), the mismatch effects can be plotted as presented in Fig. 4a-4c, by varying two parameters simultaneously in order to observe their correlations with IRR variations. Those figures can be interpreted as follows: First, in Fig. 4a, the result implied that the half-band rejection of the quadrature generator is dominant in the IRR performance with respect to the phase error of the LO. A high order quadrature generator can relax the phase error of the LO (similar effect also happens with the gain error). Clearly, it is a trade-off between power consumption and image-rejection; thus, optimization should be done to obtain a balanced point between them, matter

$$IRR = \frac{A_{ii}A_{qq}[\frac{A_{ii}}{A_{qq}}\beta\eta^2 + 2\mu\eta\ (1+\varepsilon) + \frac{A_{qq}}{A_{ii}}\lambda\ (1+\varepsilon)^2] + A_{iq}A_{qi}[\frac{A_{iq}}{A_{qi}}\lambda\eta^2 + 2\mu\eta\ (1+\varepsilon) + \frac{A_{qi}}{A_{iq}}\beta(1+\varepsilon)^2]}{A_{ii}A_{qq}[\frac{A_{ii}}{A_{qq}}\beta\eta^2 - 2\mu\eta\ (1+\varepsilon) + \frac{A_{qq}}{A_{ii}}\lambda\ (1+\varepsilon)^2] + A_{iq}A_{qi}[\frac{A_{iq}}{A_{qi}}\lambda\eta^2 - 2\mu\eta\ (1+\varepsilon) + \frac{A_{qi}}{A_{iq}}\beta(1+\varepsilon)^2]} \qquad (8)$$
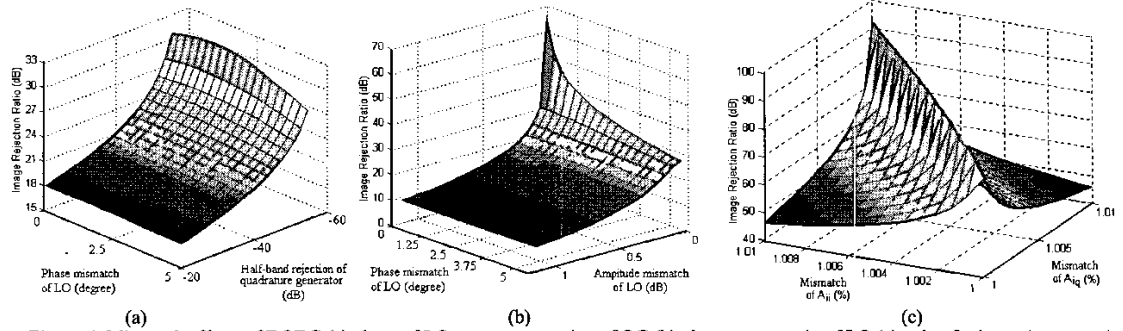
Figure 4. Mismatch effects of DQDC (a) phase of LO versus attenuation of QG (b) phase versus gain of LO (c) gain of mixers A_{ii} versus A_{iq}

that will be analyzed in the next section. The relationship between the LO amplitude and phase errors in the IRR is plotted in Fig. 4b, the figure shows that the IRR decays dramatically for both the gain and phase matching accuracies. Moreover, when the amplitude error is large, it dominates the whole IRR; this means that a further increase of phase accuracy will not improve IIR, significantly. Thus, these two parameters are relevant to each other, and should be controlled in parallel. In Fig. 4c, the relationship showed the amplitude mismatch between mixers A_{xx} $(xx=ii,iq,qi,qq)$ should be smaller than 1% to achieve IRR>45dB, which is generally insufficient to fulfill most wireless communication standards requirements. Then, this implies that this mismatch effect is the bottleneck of the entire DQDC to accomplish high image-rejection.
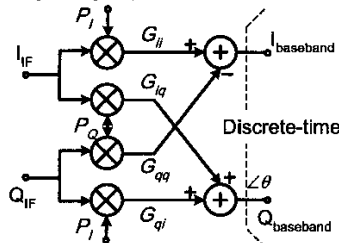

Figure 5. Non-ideal model of A-DQS scheme

2.3. Analog-Double *Q*uadrature Sampling (A-DQS)

The final frequency down-conversion from IF-to-baseband is performed by A-DQS. With the sampling frequency f_s=4xIF such A-DQS can be effectively embedded in the sample-and-hold unit of the A/D converters. Thus, prior to the A/D conversion, the signal is shifted to the baseband through complex sampling in order to employ only lowpass noise shaping $\Sigma\Delta$ A/D converters. Thus, highly reducing the complexity of the circuitries and power consumption. Regrettably, analog circuits suffer unavoidable *I/Q* mismatch, resulting in serious image problems. Then, a non-ideal model of the A-DQS scheme must be defined, as it is shown in Fig. 5.
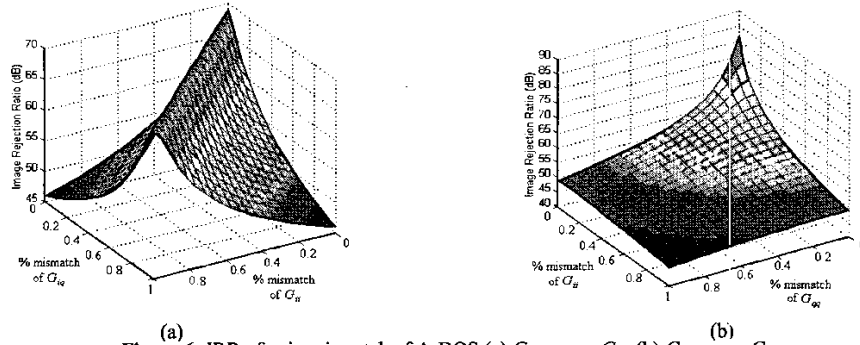
The P_I and P_Q are the complex samplers. Denoting the amplitude mismatch in the four paths as G_{ii}, G_{iq}, G_{qi} and G_{qq}. The IRR can be given by [6]

$$IRR = \frac{(G_{ii} + G_{qi} + G_{iq} + G_{qq})^2}{2(G_{ii} - G_{iq})^2 + 2(G_{qi} - G_{qq})^2} \qquad (9)$$

The mismatch relation is plotted in Fig. 6a and 6b in terms of IRR within 1% amplitude mismatch. The result implies that the required matching accuracy is relatively high, for example, with 1% amplitude mismatch; the IRR is limited to around 40dB. In the case of phase mismatch (θ), it is possible to approximate it to

$$IRR = \frac{1}{\tan^2(\theta/2)} \approx \frac{1}{(\theta/2)^2} \qquad (10)$$

For 1° phase mismatch, the IRR is limited to 41dB. Finally, as a result, both amplitude and phase mismatches of the A-DQS are critical parameters and are also modeled in this paper.

3. SIMULATION RESULTS

According to the previous analysis (with the corresponding) deduced equations and assuming as the target of total image-rejection the value of 70dBc, an optimization was conducted in MATLAB™ environment to find the optimum combination of *I/Q* mismatches among the different functional blocks, as listed in TABLE 1. The verification was conducted in SIMULINK™ by non-ideal model simulation [7]. As listed in TABLE 2, a general mismatch case is first simulated (with simulation parameters based on DCS-1800 communication standard) to verify the criticality of the modeled parameters. Then, Supposing that the inputs are two band-limited phase modulated RF signals, given by

$$X_{RF}(t) = SIG\cos[\omega_{SIG}t + \varphi_{SIG}(t)] + IMG\cos[\omega_{IMG}t + \varphi_{IMG}(t)] \qquad (11)$$

where *SIG* and *IMG* stand for the desired signal and its relative image interference, respectively. Their frequency relationship is $\omega_{SIG} = \omega_{IMG} + 2\omega_{IF}$. The normalized power spectrum densities (PSD) of the inputs (the desired one and its image interference)
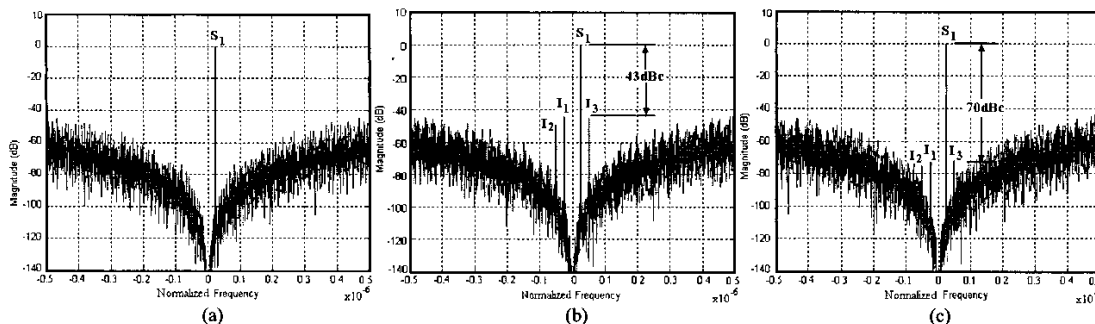

Figure 6. IRR of gain mismatch of A-DQS (a) G_{iq} versus G_{qq} (b) G_{ii} versus G_{qq}

Figure 7. Simulated PSD (a) no mismatch (b) assuming the general case (c) optimum combination, as listed in TABLE 1

are shown in Fig. 7a and b for the ideal case and general case, respectively. The desired signal is denoted as S_1 whereas its self-image is I_1. On the other hand, I_2 and I_3 are the interference and its image, respectively. The IRR is limited to approximate 43dBc as expected. Nevertheless, by applying the optimized mismatch data from TABLE 1, the achieved IRR can be approximate to 70dBc, as shown in Fig. 7c. This leads to the conclusion that the modeled parameters are dominant, which will imply later a careful design having them in a significant consideration.

4. PRACTICAL CONSIDERATIONS

The previous section as shown that the optimized combination could achieve approximate 70dBc of IRR with minimum matching requirements on each functional block. However, practical considerations are mandatory to determine the practicability of both optimized combinations, especially in CMOS implementation. The result can be discussed as follows:

Comparing with the general case, the mismatch of ΔG_{xx} in the optimum case can be tolerated up to 1.53% by increasing the half-band rejection of the quadrature generator up to 60dB and decreasing the other parameters allowable mismatches. First, 60dB half-band rejection on the entire 80MHz downlink band of DCS-1800 standard can be achieved by a 4th order RC-CR polyphase filter as mentioned in [8]. This translates to a 12dB signal power loss; thus, the output buffers of the quadrature generator in the signal path should compensate such losses by providing approximate 12dB signal gain. This leads to a power consumption of approximate 150mW. Second, employing a closely matched low power digital automatic gain control (AGC) circuits operating on the sampled low-frequency I- and Q- signals in the DSP can effectively eliminate the mixers amplitude mismatch (ΔA_{xx}) [1]. Third, 0.5dB gain and $2°$ phase imbalances of the LO translates to around 35dB half band

Table 1‡. Optimized combination of allowable mismatches in each functional blocks for IRR≈ 70dBc

Λ	α	$\varepsilon^`$	ΔA_{xx}	ΔG_{xx}	θ
58.5dB	0.48dB	1.95°	0.7%	1.53%	0.82°

Table 2‡. Simulation parameters based on DCS-1800 standard

Signal frequency	1840.2MHz
Image frequency	1827.4MHz
Local oscillator frequency	1833.8MHz
Channel bandwidth (BW)	200kHz
Intermediate frequency (IF)	6.4MHz
Over sampling ratio (OSR)	64
Order of RC-CR network	2
Order of $\Sigma\,\Delta$ ADC	2

A general case					
Λ	α	$\varepsilon^`$	ΔA_{xx}	ΔG_{xx}	θ
40dB	1dB	3°	2%	2%	3°

‡where $\varepsilon^`$ is in degree of ε

rejection requirement of the quadrature generator. This can be fulfilled by a 2nd order RC-CR network with less than 80mW power consumption in the buffers [9]. Thus, recent research showed that those obtained results should be practically realizable in today's state-of-the-art of CMOS.

5. CONCLUSIONS

A full-analytical modeling approach of I/Q mismatch effects has been presented by exploring the correlation of the receiver functional blocks to achieve high image-rejection with reasonable power consumption. By utilizing a novel complex-IF wireless receiver topology as a present model, an optimum combination of an allowable mismatch in each functional block is obtained through the theoretical analysis and the deduced equations. As a result, the required matching accuracy of the functional blocks can be traded with each other according to the power budget and image-rejection requirement. Such optimum combination is verified by non-ideal model simulation and discussed for their practicability in CMOS implementation. Hence, the image-rejection performance of complex-IF receiver can be effectively improved without adding extra circuitry.

REFERENCES

[1] Jan Crols and M. Steyaert "A Single-Chip 900MHz CMOS Receiver Front-End with a High Performance Low-IF Topology," in *IEEE JSSC*, pp.1483-1492, vol.30, No. 12, December 1995.

[2] M. Steyaert, *et al.* " A Single-chip CMOS Transceiver for DCS-1800 Wireless Communications," *IEEE ISSCC, Digest of Tech. Papers*, pp.48-49, February 1998.

[3] Jan Crols and M. Steyaert, "Low-IF Topologies for High-Performance Analog Front Ends of Fully Integrated Receivers," *IEEE Transactions on Circuits and System II:* pp.269-282, vol. 45, No. 3, March 1998.

[4] W. Sheng, *et al.* "A 3-V 0.35-μm CMOS Bluetooth Receiver IC," in *IEEE JSSC*, pp.30-42, vol.38, No.1, January 2003.

[5] Kong-Pang Pun, J. Franca, and C.A. Leme "A Quadrature Sampling Scheme with Improved Image-rejection for Complex-IF Receivers," in *Proc. IEEE ISCAS*, pp.45-48, vol.1, Sydney, Australia, May 2001.

[6] H. Kobayashi, *et al.* "Explicit transfer function of RC Polyphase Filter for Wireless Transceiver Analog Front-End," in *Proc. of IEEE Asia-Pacific. Conf. on ASIC*, pp.137-140, August 2002.

[7] Pui-In Mak *et.al.*, "*I/Q* Imbalance Modeling of Quadrature Transceiver Analog Front-Ends in SIMULINK," to appear soon in *Proc. of the IEEE Int. Conf on VTC*, October 2003.

[8] F. Behbahani, *et al.* "CMOS Mixers and Polyphase Filters for Large Image-rejection," *IEEE JSSC*, pp.873-887, vol.36, No.6, June 2001.

[9] M. Steyaert, *et al.* "Low-Voltage Low-Power CMOS-RF Transceiver Design," *IEEE Trans on Microwave Theory and Tech.*, pp.281-287, vol.50, No.1, January 2002.